Research Article

Journal of RAMAN SPECTROSCOPY

Received: 23 March 2011 Accepted: 26 April 2011 Published online in Wiley Online Library: 30 June 2011

(wileyonlinelibrary.com) DOI 10.1002/jrs.3001

Local structural order in carbonic acid polymorphs: Raman and FT-IR spectroscopy

Christian Mitterdorfer,[a] Jürgen Bernard,[a,b] Frederik Klauser,[a] Katrin Winkel,[a,b] Ingrid Kohl,[b] Klaus R. Liedl,[b] Hinrich Grothe,[c] Erwin Mayer[b] and Thomas Loerting[a]*

Two different polymorphs of carbonic acid, α- and β-H_2CO_3, were identified and characterized using infrared spectroscopy (FT-IR) previously. Our attempts to determine the crystal structures of these two polymorphs using powder and thin-film X-ray diffraction techniques have failed so far. Here, we report the Raman spectrum of the α-polymorph, compare it with its FT-IR spectrum and present band assignments in line with our work on the β-polymorph [*Angew. Chem. Int. Ed*. 48 (2009) 2690–2694]. The Raman spectra also contain information in the wavenumber range ~90–400 cm^{-1}, which was not accessible by FT-IR spectroscopy in the previous work. While the α-polymorph shows Raman and IR bands at similar positions over the whole accessible range, the rule of mutual exclusion is obeyed for the β-polymorph. This suggests that there is a center of inversion in the basic building block of β-H_2CO_3 whereas there is none in α-H_2CO_3. Thus, as the basic motif in the crystal structure we suggest the cyclic carbonic acid dimer containing a center of inversion in case of β-H_2CO_3 and a catemer chain or a sheet-like structure based on carbonic acid dimers not containing a center of inversion in case of α-H_2CO_3. This hypothesis is strengthened when comparing Raman active lattice modes at <400 cm^{-1} with the calculated Raman spectra for different dimers. In particular, the intense band at 192 cm^{-1} in β-H_2CO_3 can be explained by the inter-dimer stretching mode of the centrosymmetric $RC(OHO)_2$ CR entity with R=OH. The same entity can be found in gas-phase formic acid (R=H) and in β-oxalic acid (R=COOH) and produces an intense Raman active band at a very similar wavenumber. The absence of this band in α-H_2CO_3 confirms that the difference to β-H_2CO_3 is found in the local coordination environment and/or monomer conformation rather than on the long range.

Keywords: carbonic acid; polymorphism; center of inversion; rule of mutual exclusion; crystal structure building blocks

Introduction

Carbonic acid and its acid–base system $CO_2/H_2O \rightleftarrows H_2CO_3 \rightleftarrows HCO_3^-/H^+$ are of fundamental importance in many fields[1] including astrophysics,[2–15] medicine,[16–19] marine chemistry[20–22] and geochemistry.[23,24] Synthesis and characterization of the intermediate carbonic acid (H_2CO_3) was long believed to be impossible owing to the two decay channels to carbon dioxide and bicarbonate. In spite of that, different routes to solid and gaseous carbonic acid have been established in the last two decades.[1] Also, in aqueous solutions, trace amounts of H_2CO_3 were detected and characterized using spectroscopic techniques.[25–27] Gas-phase carbonic acid was detected following the thermolysis of NH_4HCO_3 by means of mass spectrometry,[28] following the application of a high-voltage pulse to wet CO_2 gas and supersonic jet expansion by means of FT-microwave spectroscopy[29,30] and very recently following the sublimation of pure solid H_2CO_3 by means of matrix isolation FT-IR spectroscopy.[31] Pure solid H_2CO_3 is accessible by five different techniques: (1) high-energy H or He irradiation of CO_2/H_2O ice mixtures,[3,32–35] (2) high-energy UV irradiation of CO_2/H_2O ice mixtures,[36] (3) H implantation in pure CO_2 ice,[34,37] (4) the reaction of non-energetic OH radicals with CO[38] and (5) acid–base chemistry in both (a) aqueous and (b) methanolic solution at cryo temperatures.[5,8,14,39–43] As a surface-adsorbed species, carbonic acid was also identified on carbonate minerals in acidic but dry atmosphere[44–46] and is a possible surface intermediate in the process of CO_2 adsorption on hydroxylated oxides, e.g. Fe_2O_3 or Al_2O_3.[47,48]

The main analytical tool for the detection and characterization of solid carbonic acid has been infrared spectroscopy. Techniques (1), (2), (3)[3,32–37] and (5a)[5,8,40,42] (in aqueous environment) yield practically identical infrared spectra which are assigned to crystalline β-carbonic acid. By contrast, technique (5b) (in methanolic solution) results in a distinct spectrum assigned to crystalline α-carbonic acid.[39,41,42] Other polymorphs of carbonic acid are not known at present, even though the infrared spectra obtained recently by Oba *et al*.[38] might be interpreted to be different from the spectra of the α- and β-forms. The formation of these two crystalline polymorphs from solution is preceded by the formation of two distinct amorphous forms, in which the hydrogen-bond connectivity and conformational state are similar to the crystalline forms[43] – reflecting Ostwald's step rule. The process of crystallization from the amorphous forms

* *Correspondence to: Thomas Loerting, Institute of Physical Chemistry, University of Innsbruck, Innrain 52a, A-6020 Innsbruck, Austria. E-mail: Thomas.Loerting@uibk.ac.at*

a *Institute of Physical Chemistry, University of Innsbruck, A-6020 Innsbruck, Austria*

b *Institute of General, Inorganic and Theoretical Chemistry, University of Innsbruck, A-6020 Innsbruck, Austria*

c *Institute of Materials Chemistry, Vienna University of Technology, A-1060 Vienna, Austria*

was also followed by powder X-ray diffraction.[43] However, the quality of the powder diffractograms in the crystalline state is currently not sufficient to solve the crystal structures of the two polymorphs using techniques such as Rietveld refinement. Thus, 'no information on either the local or long-range structure' of the carbonic acid polymorphs is known as pointed out by Tossell.[49]

Here, we report the Raman spectra of α- and β-carbonic acid in the range ~90–4000 cm^{-1}. This is a continuation of our recent Raman study on amorphous and β-carbonic acid, which aimed at the question whether amorphous and/or β-carbonic acid might be present on the icy parts of the Mars surface.[14] Raman spectra of α-carbonic acid are presented here for the first time, and the Raman spectra of β-carbonic acid are extended to lower wavenumbers. Raman and IR spectra yield complementary information, as IR-forbidden transitions may be Raman active and vice versa. This is called 'The rule of mutual exclusion'[50–54] and obeyed strictly in case of β-carbonic acid. By contrast, we here find that bands are both Raman and IR active in case of α-carbonic acid. This is suggestive of the centrosymmetric cyclic dimer as the local structural motif in β-carbonic acid and a non-centrosymmetric motif in α-carbonic acid. Based on the observed band positions and on the observation of needle-like crystals under the light microscope, we suggest a chain-like catemer motif or a sheet-like motif for α-carbonic acid. This finding is supported by normal mode analysis in dimeric carbonic acid units. Whereas we have focused on the 400–4000 cm^{-1} region in our earlier study, the comparison with theory focuses on the low wavenumber region at <400 cm^{-1} here. In addition, also a comparison with other carboxylic acids such as oxalic acid or malonic acid is presented.

Experimental

Solid H_2CO_3 was prepared via a cryogenic technique (5) by protonation of hydrogencarbonate anions. For details of the technique, see Refs [40,41], and for a schematic drawing of the apparatus see Ref. [55]. For the preparation of α-carbonic acid (technique 5b) methanolic solutions of 0.4 M $KHCO_3$ and 1.5 M HCl and for β-carbonic acid (technique 5a) aqueous solutions of 0.1 M $KHCO_3$ and 1 M HBr were used [$KHCO_3$ (Merck p. a.), CH_3OH (Aldrich, HPLC quality), HBr (Fluka, 48% p. a.), HCl (Supelco, 3 M in CH_3OH)]. Thin films (<4 µm) of crystalline carbonic acid were prepared by alternately vitrifying droplets of the acidic and basic solutions on optical CsI windows (13 × 2 mm) held at 77 K. By heating the films *in vacuo* (~10^{-7} mbar) to 200 K (methanolic solution) or 220 K (aqueous solution), the protonation of $KHCO_3$ takes place and the solvent and excess acid are removed from the window. To confirm the removal of the solvent and formation of crystalline carbonic acid, infrared spectra were recorded *in situ* in transmission. For this purpose, the beam passes through two KBr windows (49 × 6 mm) sealing the vacuum chamber and the sample on the CsI window inside the chamber. IR spectra were recorded on a Varian Excalibur FT-IR spectrometer at 4 cm^{-1} resolution, by co-adding 100 scans.

After breaking the vacuum, the CsI window with the H_2CO_3 film was transferred under liquid nitrogen to a precooled (~80 K) microscope cryostat (Microstat N, Oxford) in order to carry out Raman measurements, for which we employ a Labram-1B 10/78IM instrument from Dilor S.A. The excitation wavelength of 632.8 nm is supplied by a 20 mW He–Ne laser. The laser light is totally reflected by a dichroic mirror (Super Notch Plus filter) through a quartz window of the cryostat towards the sample placed below an Olympus BX 40 microscope (using a LM Plan 50× NA 0.50 objective). The Raman scattered light is collected by the microscope and totally transmitted through the notch filter towards the confocal hole and the entrance slit of the spectrometer. Then a spectrum is formed on a CCD detector. A 1800 grooves mm^{-1} grating with a resolution of ~2 cm^{-1} was used. The overall recording time for the spectra shown in Figs 1 and 2 was 7 min. The abscissa was calibrated with a silicon standard, and the sharp Raman shifts are accurate to ±2 cm^{-1} for the 1800 g mm^{-1} grating. The relative intensities of the bands in different parts of the figures are not shown on the same scale. An Oxford Microstat was used as the cryostat. The temperature of the sample was controlled by a LakeShore CI330 autotuning temperature controller and remained constant to within ±0.2 K. For imaging of the surface, a TV camera is used.

Since the crystal structure is unknown, we do not attempt an assignment of the Raman bands to normal modes of a particular symmetry type. Therefore, the assignment can only be attempted by a qualitative description of the modes, similar to that of the IR spectra of H_2CO_3 polymorphs,[3,5,32,33,36,40,41,43,56] and it is based on comparisons with assignments of other crystalline carboxylic acids and on our calculation of the harmonic wavenumbers in carbonic acid oligomers. We note that strong coupling between the various modes is often observed for carboxylic acid oligomers, which makes vibrational assignments in terms of distinct modes even less meaningful.[57–59] The vibrational spectra, including Raman and IR intensities, of carbonic acid oligomers were calculated using the Gaussian09 and Gaussian98 suite of programs. Carbonic acid dimers were calculated at a range of levels of theory, including MP2/aug-cc-pVDZ, B3LPY/6-31G(d), B3LYP/aug-cc-pVDZ and B3LYP/6-31+G(d). In this work, we pay particular attention to the Raman active modes in the range 100–500 cm^{-1}. In this range, variation of the basis set and/or method results in a shift of no more than ±5 cm^{-1}. This good performance of the hybrid density functional and the low computational cost of this method allowed us to examine also the spectra of two possible tetramer configurations.

Results

Raman spectra of α-H_2CO_3 (Fig. 1, bottom; and Fig. 2, bottom) were recorded by focusing the laser on the crystal needles (Fig. 3, top). The infrared spectrum (Fig. 1, top) was recorded directly before transferring the sample window to the Raman microstat. The vertical dashed lines are shown as a guide to the eye where the intensity is seen both in the Raman and IR in Fig. 1. Compared to the Raman spectrum of β-H_2CO_3 (reported in Ref. [14]), more bands are detected in case of α-H_2CO_3 at 500–4000 cm^{-1}. This immediately suggests a lower symmetry of the latter. The assignment of Raman bands is presented in Table 1 and is based on the assignment of IR bands presented in Ref. [41] because of the appearance of the bands in the Raman spectrum at very similar positions as in the infrared spectrum. The assignment of IR bands in Ref. [41] is itself based on IR spectra of different carbonic acid isotopologues. In addition to this assignment, we also refer to the assignment of the acid I to acid VII fundamentals presented by Wolfs and Desseyn on the example of some dicarboxylic acids.[59] We wish to stress that the assignments made in Table 1 do not imply that we are dealing with uncoupled modes. Instead, most modes are coupled with other modes, as also found in other (di)carboxylic acids such as malonic acid,[57] and so the assignments represent only qualitative descriptions.

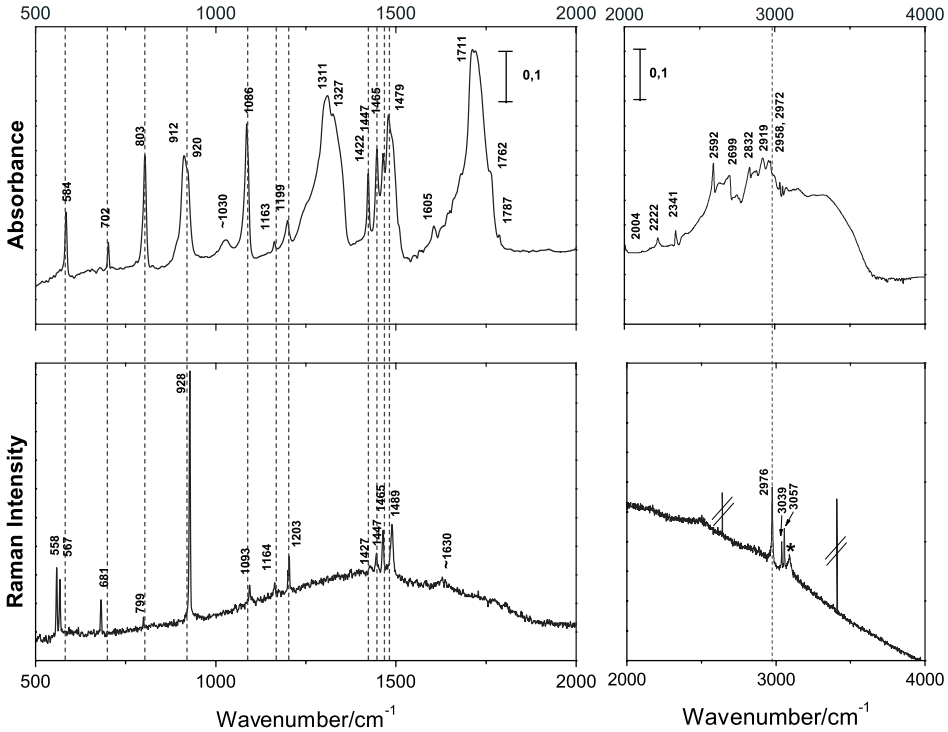

Figure 1. Comparison between FT-IR spectrum (top) and Raman spectrum (bottom) of α-H_2CO_3. The comparison between FT-IR spectrum and Raman spectrum of β-H_2CO_3 is published as Fig. 2 in Kohl *et al., Angew. Chem. Int. Ed.* **2009**, *48*, 2690.

Table 1. Raman wavenumbers (cm^{-1}) of α-H_2CO_3, made by protonation of $KHCO_3$ in methanolic solution, and their assignment

ν (cm^{-1})	Raman intensity	Assignment	Di- and polycarboxylic acids, Raman at 20 °C, Refs [59,67]
3057, 3039	m, m	ν(O–H)	
2976	s	ν(O–H)	
1630	vw	ν(C═O), acid I	1647–1782
1489, 1465, 1447, 1427	m, m, w, vw	ν_{as}[C(OH)$_2$], acid II	1367–1437
1203	m	δ(COH), acid III	1219–1275
1164	w		
1093	w	ν_s[C(OH)$_2$]	
928	vs	π(OH), δ_{oop}(COH···O), acid IV	915–950 (IR)
799	w	δ_{oop}(CO_3)	
681	m	δ(COO), acid V	641–684
567, 558	s, s	ρ(COO), δ_{ip}(CO_3), acid VI	442–601
149			
134			
113			

Low wavenumber modes (<400 cm^{-1}) are listed in Table 3. Spectra were recorded at ~80 K and ~10 mbar.

In the OH stretching region, we find two intense Raman bands at 3057 and at 3039 cm^{-1} as well as a very strong band at 2976 cm^{-1}, which we detect as weak bands in the IR. By contrast, we cannot find the IR overtones at 2701 and 2593 cm^{-1} in the Raman spectrum.[41] The absence of overtones in the Raman spectrum was expected because only a very small fraction of photons is scattered inelastically in the Raman process. The abscence of these bands, therefore, corroborates the earlier assignment of these IR bands to overtones and combination bands (see Table 1 in Ref. [41]). We attribute the Raman band centered in Fig. 1 at ~3090 cm^{-1} to the O–H stretching vibration of hexagonal ice (ice *Ih*)[60] that had condensed onto the film during the transfer of the film and the disk from the IR apparatus to the Raman microstat. Also, the translational mode of ice *Ih* centered at 225 cm^{-1} is detected in this film (Fig. 2, bottom).[61,62] The band at ~3090 cm^{-1} is also observable in the Raman spectra of D_2CO_3 samples (not shown) and shows a significantly higher full width at half-maximum, which is consistent with our assignment of this band to ice *Ih*. We note that the carboxylic acid OH stretching bands are generally weak in the Raman spectrum.[58] Whereas we were unable to detect it reliably in case of β-H_2CO_3,[14] we did detect (at least) three sharp bands in case of α-H_2CO_3. We interpret these bands due

Journal of RAMAN SPECTROSCOPY

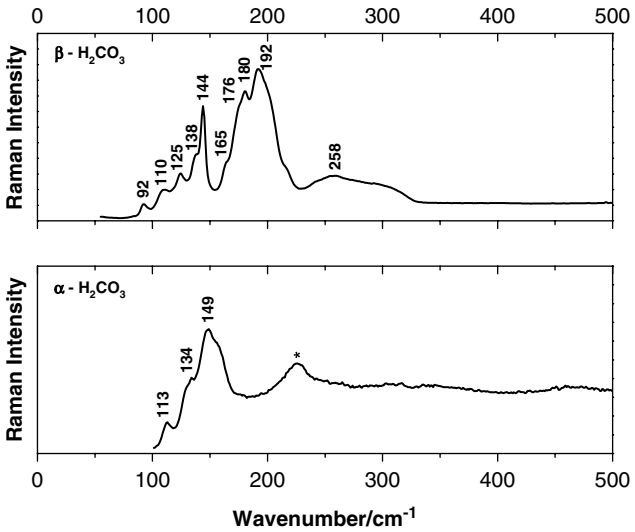

Figure 2. Low wavenumber Raman modes (<500 cm^{-1}) in β-H_2CO_3 (top) and α-H_2CO_3 (bottom).

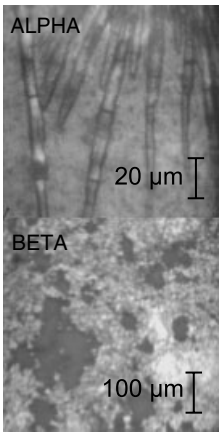

Figure 3. Microscopy images of α-H_2CO_3 (top) and β-H_2CO_3 (bottom). The images were recorded at 80 K in the Raman microstat using the confocal Raman microscope equipped with a 50× ULWD objective. Raman spectra of α-carbonic acid as depicted in Figs 1 and 2 were obtained only when focusing directly on the needles, whereas no bands at all were obtained when focusing slightly beneath the needles. Raman spectra of β-carbonic acid as shown in Fig. 2 and in Ref. [14] were obtained by focusing the laser on the dark sites.

to the OH groups in (at least) three different environments, two of which might be similar because of the very small wavenumber shift and one being inherently different. Tentatively, we assign two weakly intermolecular-bonded OH groups and one more strongly hydrogen-bonded OH group at lower wavenumbers. The picture of two weakly interacting catemer chains appears. Every chain has the same kind of intrachain hydrogen bonds and OH groups sticking out alternatingly to the left and right of the chain direction. These OH groups might loosely interact with the neighboring chains, therebye producing sheets of carbonic acid.

The intense and structured carbonyl stretching band in the IR spectrum of α-H_2CO_3 is centered at 1711 cm^{-1}. The C═O stretching mode is observed typically in the 1780 cm^{-1} region for isolated carboxylic acids and is shifted to 1720 cm^{-1} on hydrogen-bond formation.[59] In the Raman spectrum, the C═O stretch is typically observed at much lower intensity in most carboxylic acid polymorphs[59] and shifted to lower wavenumbers. The difference, which is also referred to as factor-group splitting, is typically on the order of 30–50 cm^{-1}. In case of carbonic acid, we observe a very weak Raman band at ~1630 cm^{-1}, which implies a splitting $\Delta\nu$(C═O) of ~80 cm^{-1}. The large splitting between the Raman ν_sC═O mode and the IR ν_{as}C═O mode is characteristic for carboxylic acid dimers[59] and has been examined theoretically for the formic acid dimer.[63,64] The $\Delta\nu$(C═O) value ~80 cm^{-1} is consistent with splittings obtained in various calculations of the carbonic acid dimer.[14,65] If the carbonyl group in the acid were not hydrogen-bonded or formed only (an) internal hydrogen bond(s), then one would expect a band in the range 1705–1760 cm^{-1} in both the IR and Raman spectra.[66,67] The absence of the Raman band in this region and the large splitting are strong indications for the presence of a dimer or a longer polymeric chain in α-H_2CO_3. Different polymorphs of di- and polycarboxylic acids such as oxalic acid, malonic acid or citric acid show the Raman active antisymmetric stretch ν(C═O) at 1647–1782 cm^{-1}.[59,67] As a consequence of the OH group directly connected to the carboxyl group rather than a carbon atom, both α-H_2CO_3 (1630 cm^{-1}) and β-H_2CO_3 (1608 cm^{-1}) show weak Raman bands at even lower wavenumbers. We, therefore, assign this band as the acid I band in Table 1 and suggest a chainlike catemer motif for α-H_2CO_3.

The simultaneous appearance of bands in the Raman and IR is best evidenced at 500–1500 cm^{-1}. All bands observed in the Raman spectrum in this region can also be observed at very similar positions in the IR. These are marked by vertical dashed lines in Fig. 1. Bandsplitting is apparent in both IR and Raman spectra, especially in the COH deformation region between 1430 and 1490 cm^{-1}, where four bands separated by approximately 20 cm^{-1} are observed in both spectra. Also, this band system falls outside the range typically seen in other carboxylic or dicarboxylic acids, namely 1367–1437 cm^{-1} (*cf* Table 1). This might again be explained in terms of the second OH group directly attached to the C═O group, and so we assign these bands as the acid II bands. Bands at 1203 and 1164 cm^{-1} are intense in Raman but weak in the IR. The intense IR band at 1087 cm^{-1} has a Raman counterpart at 1093 cm^{-1}. The most intense Raman band at 928 cm^{-1} can be attributed to the split band in the IR spectrum at 912/920 cm^{-1}. The IR active band at 803 cm^{-1} has its counterpart at 799 cm^{-1} in the Raman. The Raman bands in the skeletal region at 681 cm^{-1} and the doublet at 567 and 558 cm^{-1} are shifted by *ca.* +20 cm^{1} to 702 and 584 cm^{-1}. The latter band is only resolved as a doublet in the Raman but not in the IR. All these coincidences between Raman and IR clearly show that the principle of mutual exclusion does not hold in case of α-H_2CO_3, in contrast to the situation in β-H_2CO_3.[14] A local center of inversion and the cyclic centrosymmetric dimer of carbonic acid (depicted in Fig. 4(a)) can clearly be ruled out to be the building block of α-H_2CO_3, whereas we suggest this dimer to be the building block of β-H_2CO_3.[14] The large factor-group splitting in case of α-H_2CO_3 suggests that other types of dimers, oligomers or chainlike structures rather than well-separated monomers build α-H_2CO_3. We also want to emphasize that we have interpreted the IR spectra to indicate the presence of two different conformational or H-bonded states of carbonic acid.[41] This assessment has been based on the observation of two intense IR band systems assignable to the asymmetric COH stretching modes, namely at 1311/1327 cm^{-1} and 1422/1447/1465/1479 cm^{-1}, respectively (Fig. 1, top). In the Raman spectra, only the latter band system,

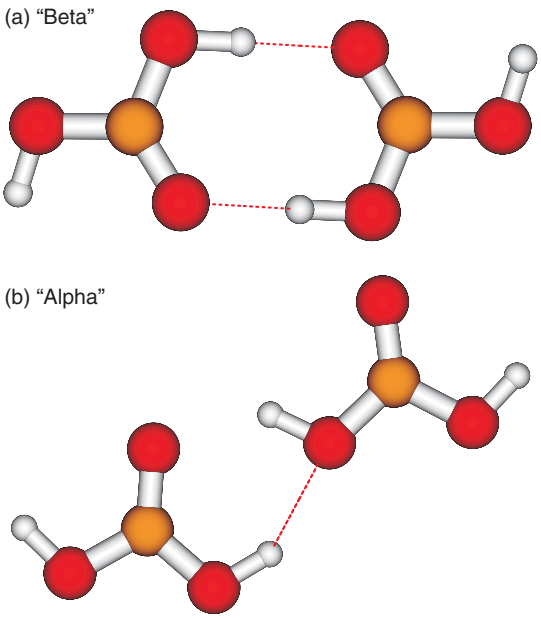

Figure 4. (a) Local structural motif suggested for β-H_2CO_3 containing a center of inversion (C_{2h} point group). (b) Candidate local structural motif suggested for α-H_2CO_3 without a center of inversion (C_S point group symmetry).

but not the former, is observed. We explain this in terms of at least two carbonic acid entities in the primitive unit cell, and we assume that this is due to an element of symmetry in the unit cell other than a center of inversion. If we follow the picture of two catemer chains connected by weak interchain hydrogen bonds, then there are two different $C(OH)_2$ stretch vibrations in every chain: one with two hydrogen-bonded OH groups, and the other with one hydrogen-bonded OH group. We expect the completely interconnected $C(OH)_2$ group at lower wavenumbers and an increase of the full width at half-maximum due to the interaction, as observed in the FT-IR spectra. At the same time, we expect a stronger change of the symmetry for these groups. This might be the reason for its disappearance in the Raman spectra, in accordance with the symmetry selection rules.

Murillo *et al.*[68] have suggested a large number of different dimers, which might serve as the fundamental dimeric unit building such a catemer chain. We have selected among these some energetically rather low-lying dimers, which are capable of producing chainlike structures and which do not show a center of inversion. One candidate structure, which we regard as a good candidate building block of α-H_2CO_3 is depicted in Fig. 4(b). We wish to emphasize, though, that also other dimers not containing a center of inversion are possible as building blocks of α-H_2CO_3. For instance, we also regard a crystal structure built from *cis–trans* carbonic acid monomers as consistent with the Raman spectroscopic results. These monomers could build linear chains via single (stronger) hydrogen bonds connecting one OH group from the first carbonic acid molecule with the C═O group of the second carbonic acid molecule. The second OH group in each carbonic acid molecule would link one linear chain of carbonic acid molecules with the other by forming (weaker) hydrogen bonds.

Recently, some candidate crystal structures have been predicted by Reddy *et al.*[69] and by us.[43] From the considerations mentioned above, the crystal structures shown in Figs. 1 and 5 in Ref. [69] and in Fig. 5(b) and (c) in Ref. [43] are possible candidate structures for β-H_2CO_3 but not for α-H_2CO_3. By contrast, the crystal structures in Figs. 2–5 in Ref. [69] and in Fig. 5(a) and (d) in Ref. [43] are possible candidate structures for α-H_2CO_3 but not for β-H_2CO_3. In the absence of IR and Raman solid state spectra calculated from various candidate structures, the experimental IR and Raman data do not allow us to pick a specific crystal structure as the best candidate at present. However, they allow restricting which kind of structures are possible and which are not possible from symmetry considerations.

Low wavenumber Raman spectra

It is well known that low wavenumber Raman spectra show highly characteristic patterns allowing easy discrimination between different crystals. This fingerprint information was recently employed to clearly distinguish between different solid nitric acid hydrates, including metastable polymorphs.[70,71] At $<400\ cm^{-1}$, β-H_2CO_3 shows more Raman bands than α-H_2CO_3 (see Fig. 2). This is in contrast to the situation encountered at $>400\ cm^{-1}$ (see discussion above). While we explain the higher number of Raman bands at $>400\ cm^{-1}$ in α-H_2CO_3 in terms of missing local symmetry, the low number of Raman bands at $<400\ cm^{-1}$ hints at a rather simple unit cell for α-H_2CO_3. By contrast, the unit cell in β-H_2CO_3 could be more complex and contain more carbonic acid molecules. The lower limit for internal modes in a dicarboxylic acid is around $250\ cm^{-1}$.[57] Whereas there are bands at $250–500\ cm^{-1}$ in case of β-H_2CO_3,[14] there is none in case of α-H_2CO_3. There are only four bands at 225, 149, 134 and $113\ cm^{-1}$ detected at $<400\ cm^{-1}$ in α-H_2CO_3 (see Table 3). As mentioned above, the band at $225\ cm^{-1}$ (Fig. 2, bottom) can also arise from the translational band in condensed hexagonal ice. By contrast, at least ten bands appear in case of β-H_2CO_3 in this region (see Fig. 2, top and Table 2). This includes the most intense Raman band appearing at $192\ cm^{-1}$, which is missing in α-H_2CO_3. A Raman band at $194\ cm^{-1}$ was recently detected in supersonic jet expansion studies of formic acid and attributed to the inter-monomer stretching mode in cyclic, centrosymmetric dimers of formic acid, i.e. the $RC(OHO)_2CR$ entity with R═H.[72] Also, in matrix isolation studies of gas-phase formic acid, an A_g band was found at $196\ cm^{-1}$, which was attributed to this mode.[73] The cyclic centrosymmetric dimer of carbonic acid contains the same $RC(OHO)_2CR$ subunit with R═OH, and so this band might be attributed to the inter-monomer stretch in the cyclic dimer of C_{2h} symmetry (see Fig. 4(a)). Indeed, we calculate the Raman active inter-monomer normal mode of A_g type to be $190 \pm 2\ cm^{-1}$ at B3LYP and MP2 levels of theory using 6–31 + G(d) or aug-cc-pVDZ basis sets from the geometry shown in Fig. 4(a). We thus suggest the mode at $192\ cm^{-1}$ observed in β-H_2CO_3 (Fig. 2, top) to be the inter-monomer stretching mode. Also, the intense modes observed at 165 and $125\ cm^{-1}$ agree very well with the predicted Raman modes at 166 ± 4 and $125 \pm 5\ cm^{-1}$ (see Table 2). By contrast, the modes at 176, 144 or $110\ cm^{-1}$ are not predicted from this simplified gas-phase calculation and might necessitate consideration of larger clusters, inclusion of crystal symmetry and a proper description of the crystal field. The mode at $144\ cm^{-1}$, for instance, appears in our calculation of the centrosymmetric carbonic acid tetramer (see Table 2). Calculation of vibrational spectra for all at least 200 different candidate crystal structures[43] are, however, not feasible.

The harmonic frequency calculations on the dimer depicted in Fig. 4(b) show two Raman active bands in the range

Journal of RAMAN SPECTROSCOPY

Table 2. Low wavenumber Raman modes (cm^{-1}) of β-H_2CO_3 obtained at ~80 K

Experimental ν (cm^{-1})	Raman intensity	Calculated (Fig. 4(a))	β-Oxalic acid Ref. [76]
258	m, br		
192	vs	190 ± 2 (A_g)	189 (A_g)
176	s		167/187 (B_g)
165	sh	166 ± 4 (A_g)	159 (A_g)
144	s		
138	sh		
125	?	121 ± 2 (B_g)	131 (B_g)
110	?		
92	?		

Note that experimental Raman intensities decay considerably at <150 cm^{-1} because of the use of a strong filter for the intense Rayleigh scattering (at 0 cm^{-1}). Calculated wavenumbers refer to gas-phase calculations in the harmonic approximation for the geometry depicted in Fig. 4(a). Error bars are given from a comparison of B3LYP and MP2 calculations and a comparison of different basis sets. Data at 300 K are from Ref. [76] and are corrected by +10 cm^{-1} in order to correct for the temperature change from 300 K to ~80 K.

Table 3. Low wavenumber Raman modes (cm^{-1}) of α-H_2CO_3 obtained at ~80 K

Experimental ν (cm^{-1})	Raman intensity	Calculated (Fig. 4(b))	α-Oxalic acid Ref. [76]
225	m, br	220 (A′)	
149	vs		161
134	s	135 (A′)	127/138
113	m		117

Note that experimental Raman intensities decay considerably at <150 cm^{-1} because of the use of a strong filter for the intense Rayleigh scattering (at 0 cm^{-1}). Calculated wavenumbers refer to gas-phase calculations in the harmonic approximation for the geometry. Most intense bands from Ref. [76] are given (90 K data).

100–500 cm^{-1}, namely two A' modes at 135 and 220 cm^{-1}. Most noteworthy, the mode at 192 cm^{-1} is clearly absent in such type of dimer and, furthermore, the two predicted Raman bands can also be found in the measured spectrum of α-H_2CO_3 (Fig. 2, bottom and Table 3). We wish to emphasize that the observed mode at 225 cm^{-1} might also arise from hexagonal ice condensed during sample transfer (see above). However, the broad, tailed nature of this band is also consistent with the presence of both hexagonal ice and carbonic acid dimer translational bands. In fact, band deconvolution is consistent with two weakly separated bands producing the band shape in Fig. 2, bottom. Of course, we have also considered other types of dimers, trimers and tetramers including the non-planar T-shaped dimer similar to the structures depicted in Fig. 4 in Ref. [68]. However, none of these can explain the vibrational features in the low wavenumber Raman spectrum of β-H_2CO_3 and α-H_2CO_3 better than the structures depicted in Fig. 4(a) and (b), respectively.

The main finding of the absence of the Raman band at 192 cm^{-1} in crystal structures based on non-centrosymmetric dimers is also found in the related case of oxalic acid. Just like in carbonic acid, there are also two polymorphs in oxalic acid.[74] And just like in carbonic acid, the crystal structure of the β-polymorph is based on the centrosymmetric dimer, whereas the crystal structure of the α-polymorph is not based on the centrosymmetric motif (see Fig. 1 in Ref. [75]). The Raman spectra of both polymorphs, including the low wavenumber region, were measured by DeVillepin and coworkers.[76] The most intense Raman modes in α-oxalic acid were found at 148, 130, 121 and 110 cm^{-1} at 300 K, which shifted by +7 to +13 cm^{-1} when cooling the sample to 90 K. This compares very well with the Raman spectrum of α-carbonic acid (Fig. 2, bottom). In case of β-oxalic acid, two A_g modes are observed at 179 and 149 cm^{-1} at 300 K. The data at 90 K are not reported, but assuming a shift of +10 cm^{-1} these two modes would be at 189 and 159 cm^{-1}, in excellent agreement with the observed spectrum of β-carbonic acid (Fig. 2, top). Also the three B_g modes observed in β-oxalic acid at 121, 157 and 177 cm^{-1} are quite similar to the modes observed in β-carbonic acid (Fig. 2, top), most notably the B_g mode at 121 cm^{-1}, which also appears in the gas-phase calculation of the cyclic dimer. We, thus, conclude that the observed low wavenumber Raman spectra are also consistent with the suggestion of the centrosymmetric dimer (Fig. 4(a)) as the local motif in β-H_2CO_3 and a non-centrosymmetric dimer as the local motif in α-H_2CO_3 (Fig. 4(b)). Whether this local motif results in a sheet-like crystal structure or a chain-like catemer type one cannot be answered from the Raman data reported here and needs to be clarified in future work.

Discussion/Conclusions

In summary, we report here the Raman spectra of α-H_2CO_3 including the low wavenumber range. In addition, we report new low wavenumber Raman data for β-H_2CO_3. While this type of Raman spectra has been reported between 30 and 100 years ago for other carboxylic or dicarboxylic acids such as formic acid,[77,78], oxalic acid,[76,79–81] malonic acid[57,79,82] or acetic acid,[67] the smallest organic acid, containing only one C atom, has eluded attempts of Raman characterization until 2009.[14] Because of the possible astrophysical relevance of carbonic acid[2–15] and the possibility of exploring astrophysical objects such as Mars using Raman spectroscopy,[83–88] the data are of importance in possibly identifying α-H_2CO_3 in outer space. For this purpose, the most intense band at 928 cm^{-1} seems to be the best marker band. For comparison, the most intense band in β-H_2CO_3 is located at 1054 cm^{-1}, while there is no band close to 928 cm^{-1}. Because of the separation of >100 cm^{-1} and the high intensity of the two bands, the α- and β-polymorphs of carbonic acid can be easily discriminated by Raman spectroscopy. For comparison, the most intense Raman band in aqueous carbonic acid attributed to the C–OH stretching vibration is at 1017 cm^{-1}.[26]

The interpretation of vibrational spectra provides valuable data, in particular concerning the local short-range ordering in these polymorphs. A comparison between IR and Raman spectra reveals that the principle of mutual exclusion only holds for β-H_2CO_3 but not for α-H_2CO_3. This suggests a local center of inversion in the former and the absence of such a center in the latter. Comparison of the observed Raman spectra with gas-phase calculations of simple carbonic acid dimers (*cf.* Fig. 4) is consistent with the idea of the centrosymmetric dimer shown in Fig. 4(a) building the β-polymorph and a non-centrosymmetric dimer similar to the one shown in Fig. 4(b) building the α-polymorph. A similar situation of the cyclic, centrosymmetric $RC(OHO)_2CR$ motif is encountered in β-oxalic acid (R=COOH),[76] and interestingly its low wavenumber Raman pattern observed resembles the one

observed here for β-carbonic acid (R═OH). Most notably, the inter-monomer stretching mode is observed in both cases at approximately 190 cm^{-1}. Similarly, the inter-monomer stretching mode in gas-phase formic acid (R═H) is also observed at 194 cm^{-1}, thus confirming the assignment of the intense Raman mode in β-H_2CO_3 at 192 cm^{-1}.[72] By contrast, this mode is missing in both α-oxalic acid and α-carbonic acid. Whereas it is known that the former has a sheet-like crystal structure built from oxalic acid dimers connected by hydrogen bonds at heads and tails, we infer from the present data that a similar situation is encountered in case of α-carbonic acid. Whether α-carbonic acid can be characterized on the long range by chain-like structures or by planar or wavy sheets and which monomer conformation is present cannot be answered from the present work. All of these possibilities can be found among the predicted candidate structures for carbonic acid,[43,69] and elucidation of the crystal structure will require future work. The Raman spectra presented here constitute an important guide for the process of determining the crystal structures of the two known polymorphs of carbonic acid, which is probably one of the last fundamental small molecules for which the crystal structure is unknown.

Acknowledgements

We gratefully acknowledge discussions with Sarah L. Price and financial support by the Austrian Science Fund (project P18187) and the European Research Council (ERC Starting Grant SULIWA).

References

[1] T. Loerting, J. Bernard, *ChemPhysChem* **2010**, *11*, 2305.
[2] J. S. Lewis, D. H. Grinspoon, *Science* **1990**, *249*, 1273.
[3] N. DelloRusso, R. K. Khanna, M. H. Moore, *J. Geophys. Res. Planets* **1993**, *98*, 5505.
[4] R. K. Khanna, J. A. Tossell, K. Fox, *Icarus* **1994**, *112*, 541.
[5] W. Hage, A. Hallbrucker, E. Mayer, *J. Chem. Soc., Farad. Trans.* **1995**, *91*, 2823.
[6] J. R. Brucato, A. C. Castorina, M. E. Palumbo, M. A. Satorre, G. Strazzulla, *Planet. Space Sci.* **1997**, *45*, 835.
[7] G. Strazzulla, J. R. Brucato, G. Cimino, M. E. Palumbo, *Planet. Space Sci.* **1996**, *44*, 1447.
[8] W. Hage, K. R. Liedl, A. Hallbrucker, E. Mayer, *Science* **1998**, *279*, 1332.
[9] M. L. Delitsky, A. L. Lane, *J. Geophys. Res. [Planets]* **1998**, *103*, 31391.
[10] R. L. Hudson, M. H. Moore, *J. Geophys. Res. [Planets]* **2001**, *106*, 33275.
[11] M. H. Moore, R. L. Hudson, P. A. Gerakines, *Spectrochim. Acta* **2001**, *57A*, 843.
[12] M. H. Moore, R. L. Hudson, R. F. Ferrante, *Earth, Moon, and Planets* **2003**, *92*, 291.
[13] R. L. Hudson, *J. Chem. Educ.* **2006**, *83*, 1611.
[14] I. Kohl, K. Winkel, M. Bauer, K. R. Liedl, T. Loerting, E. Mayer, *Angew. Chem., Int. Ed.* **2009**, *48*, 2690.
[15] Z. Peeters, R. L. Hudson, M. H. Moore, A. Lewis, *Icarus* **2010**, *210*, 480.
[16] A. Khanna, N. A. Kurtzman, *J. Nephrol.* **2006**, *19*, S86.
[17] P. Swietach, R. D. Vaughan-Jones, A. L. Harris, *Cancer Metastasis Rev.* **2007**, *26*, 299.
[18] R. D. Vaughan-Jones, K. W. Spitzer, P. Swietach, *J. Mol. Cell. Cardiol.* **2009**, *46*, 318.
[19] G. Liamis, H. J. Milionis, M. Elisaf, *Drug Saf.* **2010**, *33*, 371.
[20] C. L. Sabine, R. A. Feely, N. Gruber, R. M. Key, K. Lee, J. L. Bullister, R. Wanninkhof, C. S. Wong, D. W. R. Wallace, B. Tilbrook, F. J. Millero, T.-H. Peng, A. Kozyr, T. Ono, A. F. Rios, *Science* **2004**, *305*, 367.
[21] R. A. Feely, C. L. Sabine, K. Lee, W. Berelson, J. Kleypas, V. J. Fabry, F. J. Millero, *Science* **2004**, *305*, 362.
[22] J. C. Orr, V. J. Fabry, O. Aumont, L. Bopp, S. C. Doney, R. A. Feely, A. Gnanadesikan, N. Gruber, A. Ishida, F. Joos, R. M. Key, K. Lindsay, E. Maier-Reimer, R. Matear, P. Monfray, A. Mouchet, R. G. Najjar, G.-K. Plattner, K. B. Rodgers, C. L. Sabine, J. L. Sarmiento, R. Schlitzer, R. D. Slater, I. J. Totterdell, M.-F. Weirig, Y. Yamanaka, A. Yool, *Nature* **2005**, *437*, 681.
[23] P. Glynn, *Rev. Mineral. Geochem.* **2000**, *40*, 481.
[24] J. W. Morse, R. S. Arvidson, *Earth-Sci. Rev.* **2002**, *58*, 51.
[25] R. Kruse, E. U. Franck, *Ber. Bunsenges. Phys. Chem.* **1982**, *86*, 1036.
[26] H. Falcke, S. H. Eberle, *Water Res.* **1990**, *24*, 685.
[27] K. Adamczyk, M. Premont-Schwarz, D. Pines, E. Pines, E. T. J. Nibbering, *Science* **2009**, *326*, 1690.
[28] J. K. Terlouw, C. B. Lebrilla, H. Schwarz, *Angew. Chem., Int. Ed* **1987**, *26*, 354.
[29] T. Mori, K. Suma, Y. Sumiyoshi, Y. Endo, *J. Chem. Phys.* **2009**, *130*, 204308.
[30] T. Mori, K. Suma, Y. Sumiyoshi, Y. Endo, *J. Chem. Phys.* **2011**, *134*, 044319.
[31] J. Bernard, M. Seidl, I. Kohl, E. Mayer, K. R. Liedl, O. Galvez, H. Grothe, T. Loerting, *Angew. Chem. Int. Ed.* **2011**, *50*, 1939.
[32] M. H. Moore, R. Khanna, B. Donn, *J. Geophys. Res. [Planets]* **1991**, *96*, 17541.
[33] M. H. Moore, R. K. Khanna, *Spectrochim. Acta* **1991**, *47A*, 255.
[34] J. R. Brucato, M. E. Palumbo, G. Strazzulla, *Icarus* **1997**, *125*, 135.
[35] G. Strazzulla, G. Leto, F. Spinella, O. Gomis, *Astrobiology* **2005**, *5*, 612.
[36] P. A. Gerakines, M. H. Moore, R. L. Hudson, *Astron. Astrophys.* **2000**, *357*, 793.
[37] M. Garozzo, D. Fulvio, O. Gomis, M. E. Palumbo, G. Strazzulla, *Planet. Space Sci.* **2008**, *56*, 1300.
[38] Y. Oba, N. Watanabe, A. Kouchi, T. Hama, V. Pirronello, *Astrophys. J.* **2010**, *722*, 1598.
[39] W. Hage, A. Hallbrucker, E. Mayer, *J. Am. Chem. Soc.* **1993**, *115*, 8427.
[40] W. Hage, A. Hallbrucker, E. Mayer, *J. Chem. Soc., Farad. Trans.* **1996**, *92*, 3197.
[41] W. Hage, A. Hallbrucker, E. Mayer, *J. Chem. Soc., Farad. Trans.* **1996**, *92*, 3183.
[42] W. Hage, A. Hallbrucker, E. Mayer, *J. Mol. Struct.* **1997**, *408*, 527.
[43] K. Winkel, W. Hage, T. Loerting, S. L. Price, E. Mayer, *J. Am. Chem. Soc.* **2007**, *129*, 13863.
[44] H. A. Al-Hosney, V. H. Grassian, *J. Am. Chem. Soc.* **2004**, *126*, 8068.
[45] H. A. Al-Hosney, S. Carlos-Cuellar, J. Baltrusaitis, V. H. Grassian, *Phys. Chem. Chem. Phys.* **2005**, *7*, 3587.
[46] H. A. Al-Hosney, V. H. Grassian, *Phys. Chem. Chem. Phys.* **2005**, *7*, 1266.
[47] J. Baltrusaitis, J. D. Schuttlefield, E. Zeitler, J. H. Jensen, V. H. Grassian, *J. Phys. Chem. C* **2007**, *111*, 14870.
[48] J. Baltrusaitis, V. H. Grassian, *J. Phys. Chem. A* **2010**, *114*, 2350.
[49] J. A. Tossell, *Inorg. Chem.* **2006**, *45*, 5961.
[50] T. Venkatarayudu, *J. Chem. Phys.* **1954**, *22*, 1269.
[51] A. R. H. Cole, J. R. Durig, *J. Raman Spectrosc.* **1975**, *4*, 31.
[52] R. Mendelsohn, E. U. Monse, *J. Chem. Educ.* **1981**, *58*, 582.
[53] S. F. Parker, H. Herman, *Spectrochim. Acta* **1997**, *53A*, 119.
[54] R. L. Frost, M. L. Weier, *J. Raman Spectrosc.* **2003**, *34*, 776.
[55] I. Kohl, L. Bachmann, A. Hallbrucker, E. Mayer, T. Loerting, *Phys. Chem. Chem. Phys.* **2005**, *7*, 3210.
[56] G. Strazzulla, G. A. Barratta, M. E. Palumbo, M. A. Satorre, *Nucl. Instrum. Methods Phys.Research, Sect. B* **2000**, *166–167*, 13.
[57] D. Bougeard, J. De Villepin, A. Novak, *Spectrochim. Acta* **1988**, *44A*, 1281.
[58] D. Lin-Vien, N. B. Colthup, W. G. Fateley, J. G. Grasselli, *The Handbook of Infrared and Raman Characteristic Frequencies of Organic Molecules*, Academic Press: New York, **1991**.
[59] I. Wolfs, H. O. Desseyn, *Appl. Spectrosc.* **1996**, *50*, 1000.
[60] P. T. T. Wong, E. Whalley, *J. Chem. Phys.* **1975**, *62*, 2418.
[61] M. J. Taylor, E. Whalley, *J. Chem. Phys.* **1964**, *40*, 1660.
[62] P. T. T. Wong, E. Whalley, *J. Chem. Phys.* **1976**, *65*, 829.
[63] W. L. Qian, S. Krimm, *J. Phys. Chem.* **1996**, *100*, 14602.
[64] W. L. Qian, S. Krimm, *J. Phys. Chem. A* **2002**, *106*, 11663.
[65] P. Ballone, B. Montanari, R. O. Jones, *J. Chem. Phys.* **2000**, *112*, 6571.
[66] N. B. Colthup, L. H. Daly, S. E. Wiberley, *Introduction to Infrared and Raman Spectroscopy*, Academic Press: New York, **1964**.
[67] F. R. Dollish, W. G. Fateley, F. F. Bentley, *Characteristic Raman Frequencies of Organic Compounds*, Wiley: New York, **1974**, pp 105.
[68] J. Murillo, J. David, A. Restrepo, *Phys. Chem. Chem. Phys.* **2010**, *12*, 10963.
[69] S. K. Reddy, C. H. Kulkarni, S. Balasubramanian, *J. Chem. Phys.* **2011**, *134*, 124511.
[70] H. Grothe, C. E. L. Myhre, C. J. Nielsen, *J. Phys. Chem. A* **2006**, *110*, 171.

[71] R. M. Escribano, D. Fernandez-Torre, V. J. Herrero, B. Martin-Llorente, B. Mate, I. K. Ortega, H. Grothe, *Vib. Spectrosc.* **2007**, *43*, 254.
[72] P. Zielke, M. A. Suhm, *Phys. Chem. Chem. Phys.* **2007**, *9*, 4528.
[73] A. Olbert-Majkut, J. Ahokas, J. Lundell, M. Pettersson, *Chem. Phys. Lett.* **2009**, *468*, 176.
[74] L. J. Bellamy, R. J. Pace, *Spectrochim. Acta* **1963**, *19*, 435.
[75] I. Nobeli, S. L. Price, *J. Phys. Chem. A* **1999**, *103*, 6448.
[76] J. De Villepin, A. Novak, D. Bougeard, *Chem. Phys.* **1982**, *73*, 291.
[77] S. M. Blumenfeld, H. Fast, *Spectrochim. Acta* **1968**, *24*, 1449.
[78] H. R. Zelsmann, Y. Marechal, A. Chosson, P. Faure, *J. Mol. Struct.* **1975**, *29*, 357.
[79] D. Hadzi, N. Sheppard, *Proc. Roy. Soc. (London)* **1953**, *A216*, 247.
[80] J. De Villepin, A. Novak, *Spectrochim. Acta* **1978**, *34A*, 1019.
[81] J. De Villepin, A. Novak, *Spectrochim. Acta* **1978**, *34A*, 1009.
[82] J. De Villepin, M. H. Limage, A. Novak, N. Toupry, M. Le Postollec, H. Poulet, S. Ganguly, C. N. R. Rao, *J. Raman Spectrosc.* **1984**, *15*, 41.
[83] A. Wang, L. A. Haskin, A. L. Lane, T. J. Wdowiak, S. W. Squyres, R. J. Wilson, L. E. Hovland, K. S. Manatt, N. Raouf, C. D. Smith, *J. Geophys. Res., [Planets]* **2003**, *108*, 5005.
[84] A. Ellery, D. Wynn-Williams, *Astrobiology* **2003**, *3*, 565.
[85] J. L. Bishop, E. Murad, *J. Raman Spectrosc.* **2004**, *35*, 480.
[86] J. Popp, M. Schmitt, N. Tarcea, W. Kiefer, M. Hilchenbach, T. Stuffler, S. Hofer, R. Hochleitner, A. Wuttig, R. Riesenberg, *Eur. Space Agency, [Spec. Publ.]* **2005**, *SP-588*, 385.
[87] P. Sobron, F. Sobron, A. Sanz, F. Rull, *Appl. Spectrosc.* **2008**, *62*, 364.
[88] J. Jehlicka, A. Culka, H. G. M. Edwards, *Planet. Space Sci.* **2010**, *58*, 875.